ISSN 1318-0010
KZLTET 31(6)485(1997)

GROWTH OF III-NITRIDES VIA SUBLIMATION AND METALORGANIC VAPOR PHASE EPITAXY

RAST III-NITRIDOV S SUBLIMACIJO IN METALORGANSKO PARNO FAZNO EPITAKSIJO

ROBERT F. DAVIS[1], C. M. BALKAS[1], M. D. BREMSER[1], O. H. NAM[1], W. G. PERRY[1], B. L. WARD[2], Z. SITAR[1], T. ZHELEVA[1], L. BERGMAN[2], I. K. SHMAGIN[3], J. F. MUTH[3], R. M. KOLBAS[3], R. J. NEMANICH[2]

[1]Department of Materials Science and Engineering, North Carolina State University, Box 7907 Raleigh, NC, 27695-7907
[2]Department of Physics, North Carolina State University, Box 8202, Raleigh, NC 27695-8202
[3]Department of Electrical and Computer Engineering, North Carolina State University, Box 7911, Raleigh, NC 27695-7911

Prejem rokopisa - received: 1997-10-01; sprejem za objavo - accepted for publication: 1997-10-21

Single crystals of GaN ≤ 3 mm in length were grown by sublimation/recondensation of GaN in 760 Torr NH_3 at 1100°C. Platelets of AlN ≤ 1 mm thick were similarly grown between 1950 and 2250°C using an Al source. Monocrystalline GaN and $Al_xGa_{1-x}N$(0001) ($0.05 \leq x \leq 0.96$) films were grown via MOVPE on α(6H)-SiC(0001) wafers with and without, respectively, a 1000 Å AlN buffer layer. Photoluminescence (PL) spectra of GaN showed bound and free excitonic recombinations. Selective growth of hexagonal pyramid arrays of undoped GaN and Si-doped GaN was achieved on 6H-SiC(0001)/AlN/GaN multilayer substrates using a patterned SiO_2 mask. Field emission of these arrays exhibited a turn-on field of 25 V/μm for an emission current of 10.8 nA at an anode-to-sample distance of 27 μm. Lateral growth and coalescence of GaN have been achieved using stripes oriented along <1$\bar{1}$00> at 1100°C and a triethylgallium flow rate of 26 mmol/min. Approximately 10^9 cm^{-2} dislocations, originating from the underlying GaN/AlN interface, were contained in the GaN grown in the window regions. The overgrowth regions contained a very low density of dislocations.

Key words: gallium nitride, aluminum nitride, single crystals, thin films, photoluminescence, Raman spectroscopy, cathodoluminescence, selective growth, lateral overgrowth

Kristali GaN ≤ 3 mm dolžine so bili izdelani s sublimacijo/rekondenzacijo GaN pri 760 tor. NH_3 in 1100°C. Ploščice AlN ≤ 1 mm debeline so bile na podoben način izdelane pri 1950 do 2250°C z uporabo Al kot izvora. Monokristalini filmi GaN in Al_xGa_{1-x} N(001) z ($0.05 \leq x \leq 0.96$) so bili izdelani z MOVPE na α(6H)-SiC(0001) vaferjih z in brez 1000 Å AlN bufer sloja. Fotoluminiscentni (PL) spektri GaN so pokazali vezi in proste excitonske rekombinacije. Selektivna rast združb heksagonalnih piramid nedopiranega GaN in GaN dopiranega s silicijem je bila dosežena na 6H - Si(0001)/AlN/GaN večslojnih substratih z uporabo vzorčastih SiO_2 mask. Prag polja emisije teh združb je imel jakost 25 V/μm za emisijski tok 10.8 nA pri razdalji 27 μm med anodo in preizkušancem. Lateralna rast in koalescenca GaN je bila dosežena z uporabo lamel orientiranih vzdolž <1$\bar{1}$00> pri 1100°C in pretoku trietilgalija 26 mmol/min. V GaN, ki je nastal v področju oken je bilo približno 10^9 cm^{-2} dislokacij, ki so izvirale iz mejne površine GaN/AlN. Področja večje rasti so imela majhno gostoto dislokacij.

Ključne besede: galijev nitrid, aluminijev nitrid, posamični kristali, tanki filmi, fotoluminiscenca, Raman spektroskopija, katodoluminiscenca, selektivna rast, pospešena lateralna rast

1 INTRODUCTION

The realization of blue and green light emitting diodes and blue lasers as well as prototypes of several microelectronic devices produced from GaN-based materials containing copious line and planar defects has been most fortunate. These achievements also indicate that the employment of substrates on which homoepitaxial films can be grown would result in marked improvements in the properties of the devices fabricated in these films. At present, very thin films of GaN, AlN and $Al_XGa_{1-X}N$ are deposited on foreign substrates as buffer layers on which the device-related III-V nitrides films are grown. Aluminum nitride is also a candidate material for selected piezoelectric applications and surface acoustic wave (SAW) devices. However, the potential of AlN in these and other applications has been hampered by the lack of bulk single crystals, as discussed in several review articles[1-4]. Gallium nitride is a promising material for field emission because of its low electron affinity (2.7-3.3eV)[5,6], reasonable thermal, chemical and mechanical stability and the ability for controlled n-type doping. Recently, it has been reported[6,7] that AlN and Al-rich $Al_XGa_{1-X}N$ ($x \geq 0.75$) films exhibit a negative electron affinity which suggests that these materials belong to a special class of field emitters.

Recent research conducted by the authors and described in the following sections represent important advances in the determination of the process parameters necessary to achieve growth of GaN and AlN bulk single crystals via seeded sublimation/recondensation. Additionally, we discuss the employment of a 1000 Å, monocrystalline, high-temperature (HT) (1100°C) AlN buffer layer for metalorganic vapor phase epitaxy (MOVPE) thin film deposition which has resulted in subsequently deposited GaN films void of oriented domain structures and associated low-angle grain boundaries[8,9]. Monocrystalline films of $Al_xGa_{1-x}N$ ($0.05 \leq x \leq 0.96$) of the same quality as GaN with a HT-AlN buffer layer have also been achieved directly on 6H-SiC(0001) wafers at 1100°C. We also report the selective growth of GaN and Si-doped GaN hexagonal pyramid arrays on

circular patterns etched in SiO_2 masks deposited on GaN/AlN/6H-SiC(0001) multilayer substrates and the field emission results from these arrays, as well as the deposition, the lateral overgrowth and subsequent coalescence of the GaN stripes selectively grown in the same manner.

2 EXPERIMENTAL PROCEDURES

A. GaN Bulk Growth

Growth of individual GaN crystals was achieved by evaporating 0.5" diameter and 0.25" high GaN pellets cold pressed from high purity GaN powders produced in our laboratory[10] in a stream of 99.9999% pure NH_3 gas. Experiments were conducted in a system that was specifically designed for GaN growth. The growth system consisted of: (1) an outer vacuum chamber that contained the heat shields and electrical feed-throughs and (2) a reaction tube containing the source and seed materials. Two independently controlled heaters were used to achieve the necessary temperature gradients for sublimation growth. Heater temperatures were monitored and controlled via the use of thermocouples placed adjacent to each heater. Source and substrate temperatures were monitored independently from within the reaction tube. Experiments were performed within the source temperature range of 1100-1450°C. The seed heater was maintained at 1100°C throughout each deposition. Growth pressures of 50-760 torr were investigated; however, most experiments were conducted at 760 torr. An NH_3 flow rate of 50 sccm was used for all growth experiments. Blank BN seed holders were used as substrates and placed at a distance from the source wherein the crystals with low aspect ratios could be obtained.

B. AlN Bulk Growth

Aluminum nitride sublimation/recondensation experiments were also conducted in a resistively heated graphite furnace. Bulk AlN (99% dense) blocks produced via sintering without additives were used as the source material. The source was positioned in the isothermal section of the furnace to ensure an essentially constant evaporation rate. Single crystal, 6H-SiC (0001) squares (10 mm x 10 mm) were used as seeds in all experiments due to the relatively small lattice mismatch to AlN (0.9%) and high temperature stability. The seed crystals were heated in vacuum at ≈1150°C prior to crystal growth to desorb the surface oxide, hydrocarbons and any other contaminants.

All AlN experiments were performed under a 100 sccm flow of ultra-high purity N_2. The background pressure was maintained at 500 Torr by an automatic throttle valve. The temperature ranges of 2100-2250°C and 1950-2050°C were investigated consecutively. The lower temperature range was employed primarily because of the degradation of the furnace and the seed crystals at the higher temperatures. In both cases, a temperature difference of 80-150°C was employed, depending on the separation distance (1-40 mm) between the source and the seed. The growth rate at a separation of 3 mm was ≈30 times higher than at a 15 mm separation. The AlN source was repositioned to the desired source height before each experiment.

C. Metalorganic Vapor Phase E pitaxy and Selective Area Growth

As-received vicinal 6H-SiC(0001) wafers[11] oriented 3°-4° off-axis toward <11$\bar{2}$0> were cut into 7 mm squares. These pieces were degreased in sequential ultrasonic baths of trichloroethylene, acetone and methanol and rinsed in deionized water. The substrates were subsequently dipped into a 10% HF solution for 10 minutes to remove the thermally grown oxide layer and blown dry with N_2 before being loaded onto the SiC-coated graphite susceptor contained in a cold-wall, vertical, pancake-style, MOVPE deposition system. The system was evacuated to $\leq 3 \times 10^{-5}$ Torr prior to initiating growth. The continuously rotating susceptor was RF inductively heated to the GaN ($Al_xGa_{1-x}N$) deposition temperature of 1050°C (1100°C) (optically measured on the susceptor) in 3 SLM of flowing H_2 diluent. Hydrogen was also used as the carrier gas for the various metalorganic precursors. Deposition of $Al_xGa_{1-x}N$ was initiated by flowing various ratios of triethylaluminum (TEA) and triethylgallium (TEG) in combination with ammonia (NH_3).

Selective growths of GaN and $Al_{0.2}Ga_{0.8}N$ were achieved at 1000-1050°C with TEG flow rates = 26.1-70.0 μm/min. on stripe (window width = 3-80 μm) and circular (diameter = 5 μm) patterned GaN/AlN/6H-SiC(0001) multilayer substrates. To produce these patterned substrates, a SiO_2 mask layer (thickness = 1000Å) was subsequently deposited on each GaN film via RF sputtering or low pressure chemical vapor deposition. Patterning of the mask layer was achieved using standard photolithography techniques and etching with a buffered HF solution. The edges of the stripe patterned samples were parallel to <11$\bar{2}$0>. Prior to selective growth, the patterned samples were dipped in a buffered HCl solution to remove the surface oxide of the underlying GaN layer. Incorporation of the n-type Si dopant into the GaN pyramids during growth was achieved using SiH_4 at a flow rate of 5.5 nmol/min.

Field emission measurements (FEM) were performed on the Si-doped GaN hexagonal pyramid arrays in a UHV-FEM system having a working pressure of 2×10^{-8} Torr. Each array was placed beneath a five mm diameter movable Mo anode having a flat tip. The anode was controlled by a stepping motor such that one step yielded a translation of 0.44 μm. The current-voltage (I-V) measurements were taken from 2 to 40 μm for anode voltages in the range of 0 to 1100 V.

The lateral overgrowth of GaN was achieved in a manner similar to that of the films[12]. The GaN grew vertically to the top of the mask and then both laterally and vertically over the mask until the lateral growth fronts from many different windows coalesced and formed a continuous layer. The samples were characterized by scanning electron microscopy (SEM-JEOL 6400 FE), atomic force microscopy (AFM-Digital Instrument NanoScope III) and transmission electron microscopy (TEM-TOPCON 002B, 200KV).

3 RESULTS AND DISCUSSION

A. Bulk GaN Growth

Colorless wurtzitic GaN crystals ≤ 3 mm in size were achieved by sublimation of the pressed GaN pellets in a stream of ammonia. **Figure 1** shows an optical micrograph of ≈1 mm long, well faceted, transparent GaN crystals with low aspect ratios which are in contrast to the commonly observed[13] needle-shaped crystals grown via vapor phase reaction. The GaN crystals primarily grew by spontaneous nucleation on the BN seed holders. The use of temperatures above 1200°C resulted in the rapid conversion of the GaN source into Ga metal. Crystals were grown at source temperatures in the range of 1100-1200°C; however, the majority of experiments were conducted at 1200°C to achieve higher growth rates. The temperature of the BN surface where crystals nucleated was ≈1000°C. The growth time and pressure for the growth of the crystals shown in **Figure 1** were 2.5 hrs and 760 Torr, respectively.

The direction of fastest growth and thus the crystal shape were observed to change with the changing Ga/NH_3 flux ratio and the growth temperature. These observations are in contrast to all previous reports which indicate that growth of bulk GaN from the vapor phase results primarily in long needles.

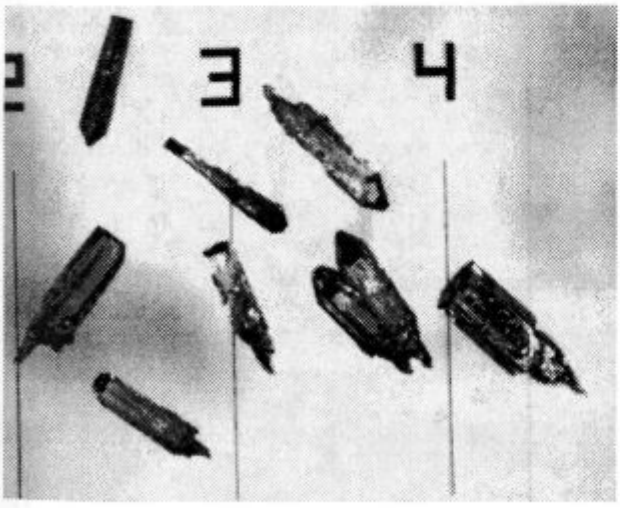

Figure 1: GaN crystals grown by sublimation/recondensation on BN. Lines are spaced 1 mm
Slika 1: GaN kristali zrastli s sublimacijo/rekombinacijo na BN. Črte so oddaljene 1 mm

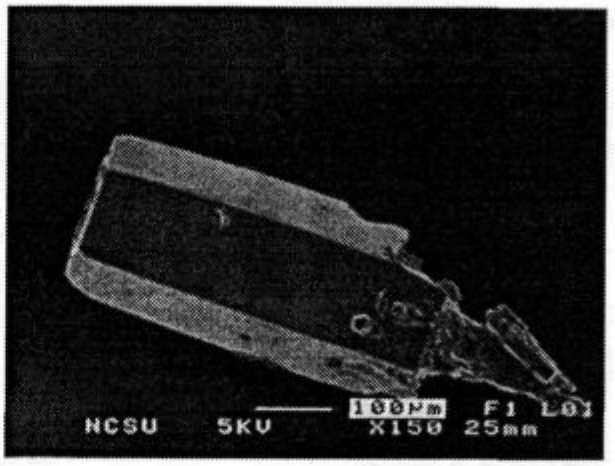

Figure 2: Secondary electron microscopy of a GaN crystal showing well developed {1010} and {0001} crystallographic facets
Slika 2: SEM posnetek GaN kristalov, ki kaže dobro razvite {1010} in {0001} kristalne ploskve

Figures 2 and 3 show SEM images of the same crystal. This crystal grew from a single isolated nucleation site and developed into a well faceted hexagonal shape terminated by flat {1010} and {0001} planes. **Figure 3** shows a higher magnification image in which the (0001) and (1010) facets are observed.

A spectral mass scan via SIMS indicated that all impurities with the exception of oxygen were at background levels. Quantitative analysis revealed an oxygen concentration of $3x10^{18}$ atoms/cm^3 which is similar to that present in high quality GaN thin films.

A representative room temperature PL spectrum for bulk GaN taken at 300K is shown in **Figure 4**. Strong near band edge (bound exciton) emission with a peak position at 365.0 nm (3.4 eV) and a FWHM of 9.0 nm (83 meV) was observed. The visible portion of the PL

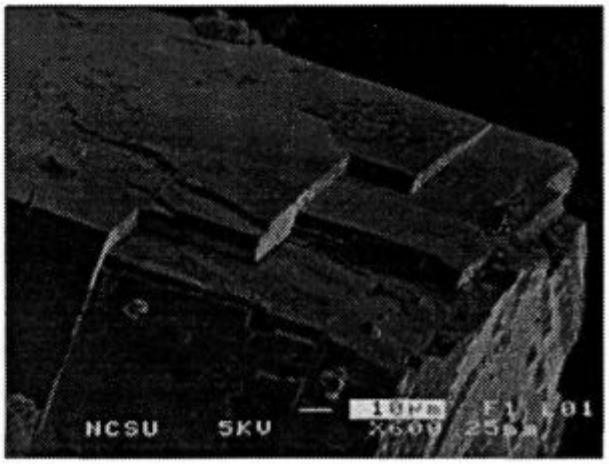

Figure 3: Higher magnification of the crystal in **Figure 2**
Slika 3: Kristal na **sliki 2** pri večji povečavi

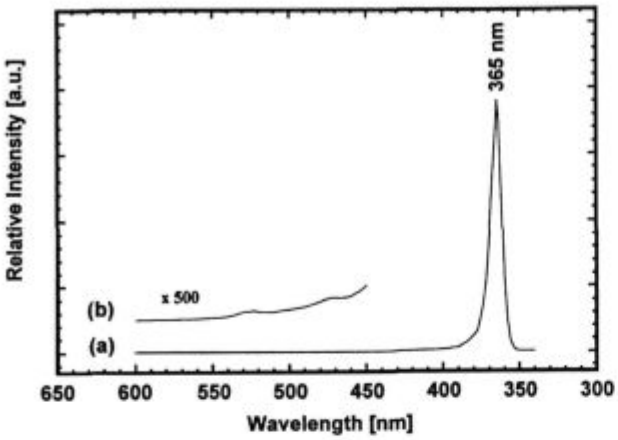

Figure 4: Photoluminescence spectrum of GaN taken at 300 K
Slika 4: Fotoluminiscentni spekter GaN pri 300 K

spectrum is expanded 500 times in the inset in **Figure 4**. No yellow emission usually attributed to deep level transitions was detected on this scale or to the naked eye. A peak position of 359.0 nm with a FWHM of 54 meV was detected for a PL spectrum obtained at 77 K.

The allowed Raman modes of the wurtzite structure are presented in **Figure 5**. The inset in this figure shows that the $E2^{(2)}$ mode is at 567 cm^{-1} and has a FWHM ≈ 3.5 cm^{-1}. These values are indicative of a material of the highest quality reported to date[14].

The results of optical absorption studies are shown in **Figure 6**. The absorption band edge is distinct but is not as sharply defined as observed in thin epitaxial films. This is due to the absorption tail below the band edge. The absorption edge is expected to shift to wavelengths above the actual band gap (360 nm for GaN) as the material thickness increases. For example, in the absorption spectrum of a high quality 50 μm thick GaN film the absorption edge is observed at 369 nm, and 75% transmission is observed at 379 nm [15]. Since the GaN crystal

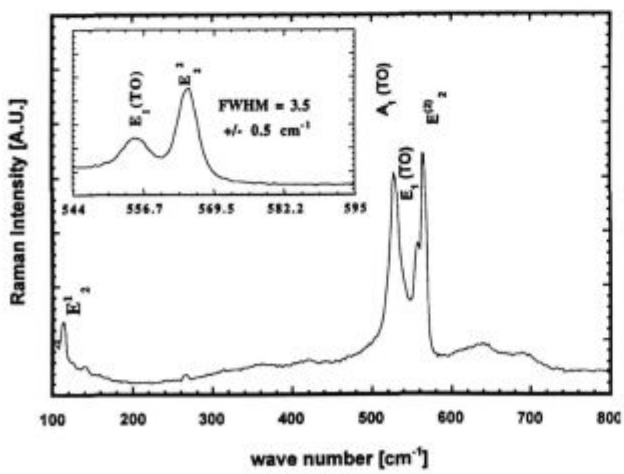

Figure 5: Raman spectrum of GaN
Slika 5: Raman spekter GaN

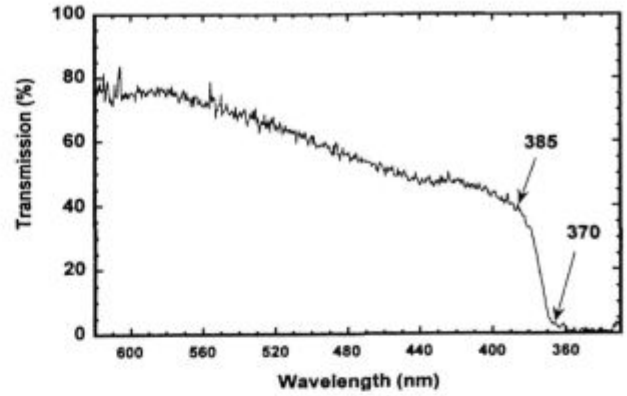

Figure 6: Optical absorption spectrum of GaN crystal
Slika 6: Optični absorpcijski spekter GaN kristala

from which the above spectrum taken was ≈ 300 μm thick, the absorption edge position of ≈ 370 nm and 75% transmission indicate these crystals to be of high optical quality.

B. AlN Bulk Growth

Growth in the 2100-2250°C range

Single crystal platelets of AlN having thicknesses to one millimeter and covering the whole seed crystal were obtained at a source temperature of 2150°C and a 4 mm source-to-seed separation. The growth rate was estimated to be 0.5 mm/hr. The results of XRD and Laue back reflection studies confirmed the monocrystallinity.

At higher growth temperatures between 2150-2250°C several ≈ 2 x 2 mm individual hexagonal crystals were obtained on the seeds, since at these temperatures, severe degradation of the SiC substrates resulted in isolated stable nucleation sites. These crystals and the aforementioned platelets ranged in color from green to blue. The coloration strongly indicated the incorporation of impurities which was confirmed via SIMS analysis to be C and Si from the SiC substrates.

Upon cooling, the AlN crystals frequently delaminated and cracked. This was most probably due to the mismatch in the coefficients of thermal expansion between the two materials; however, intrinsic stress in the deposited material and/or the extension of pre-existing cracks at the edges of the SiC substrates may also have contributed to these phenomena. Unfortunately, the thermal expansion coefficients data for these materials are not available for the entire temperature range of the experiments. Since AlN boules will ultimately be grown on obtained AlN crystals, this cracking problem should not be a significant barrier to the attainment of much larger crystals.

Growth in the 1950-2050°C range

Growth of AlN in the temperature range of 1950 to 2050°C was conducted because complete structural and chemical stability of the SiC seeds and a significant re-

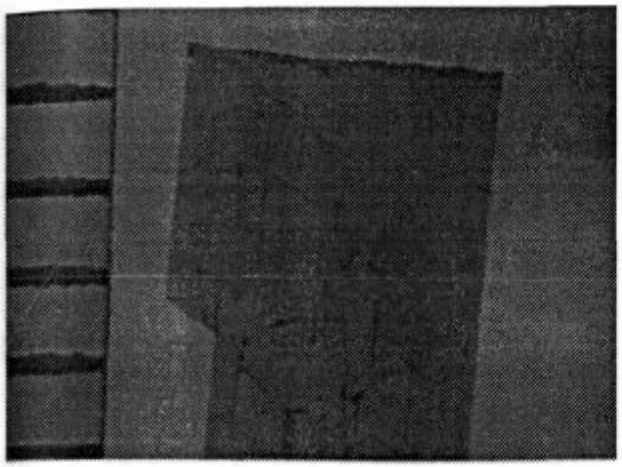

Figure 7: Optical micrograph of a single crystal of AlN grown at 1950°C and a 4 mm source-to-seed separation (Scale: mm)
Slika 7: Optični posnetek kristala AlN, ki je zrastel pri 1950°C in razdalji 4 mm med izvorom in kaljo (merilo: mm)

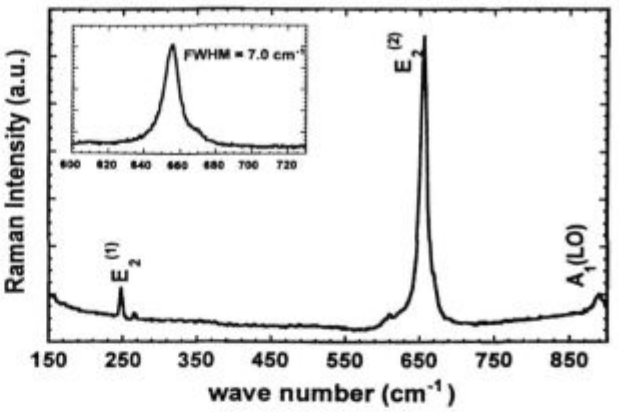

Figure 8: Raman spectrum of transparent bulk AlN grown at 1950°C
Slika 8: Raman spekter prosojnega AlN, ki je bil zraščen pri 1950°C

duction in the deterioration of the SiC coated crucibles were attained. Crystals grown in this temperature range were always colorless regardless of the morphology or growth site and contained almost two orders of magnitude less Si and C than the crystals deposited at >1950°C; whereas, the O levels were similar in all crystals. Typical growth rates were reduced to 30-50 μm/hr. Growth runs of 10-15 hrs yielded 0.3-0.5 mm thick crystals on 1 cm^2 SiC substrates. A 0.4 mm thick transparent AlN platelet grown at 1975°C can be seen in **Figure 7**. Unfortunately cracking occurred in these crystals as well and presumably for the same reasons stated in the previous subsection. Crystals grown in both temperature ranges had very smooth surfaces (– RMS = 6Å) as determined by atomic force microscopy (AFM).

All crystals showed strong and well defined single crystalline XRD patterns. Only the (002) reflection positioned at 36° was observed in symmetric È-2È scans for a crystal grown at 1950°C. This suggests that the residual stress level in these crystals was low. Bright field, plan view TEM micrographs and associated selected area diffraction (SAD) patterns taken along the [0001] direction showed uniform contrast density throughout the specimen and spot patterns without streaks or arcs, respectively, indicative of single-crystalline material without high angle boundaries, stacking faults, misoriented grains or twinned regions.

A Raman spectrum acquired using back scattering geometry from the (0001) face of an transparent AlN crystal grown at 1950°C is presented in **Figure 8**. The spectrum exhibits the allowed modes for this geometry, namely, $A_1(LO) \approx 893$ cm^{-1}, $E_2^{(1)} \approx 250$ cm^{-1}, $E_2^{(2)} \approx 660$ cm^{-1} with no detectable contribution from the forbidden modes. The results support the aforementioned crystallographic and microstructural results in that a well defined wurtzite structure exists without significant concentrations of structural defects or internal stress which could relax the selection rules. The inset shows the high resolution spectrum of the $E_2^{(2)}$ mode. The FWHM of this peak was 7.0±0.5 cm^{-1}; the same spectrum taken from a blue crystal grown at 2200°C had a FWHM value of 9.5±0.5 cm^{-1}. This marked difference complements the results of the SIMS analysis in which the colored crystals contained two orders of magnitude more Si.

C. Metalorganic Vapor Phase Epitaxial Growth of GaN and $Al_xGa_{1-x}N$ films

Previous research in our laboratories has shown that thin films of GaN deposited directly on 6H-SiC(0001) substrates at high and low temperatures had columnar-like grains, faceted surfaces and high net carrier concentrations (n_D-$n_A > 1 \times 10^{19}$ cm^{-3})[16]. In contrast, in the present research monocrystalline thin films of both the HT-AlN buffer layers and the subsequently grown GaN films deposited on similar SiC substrates have been deposited with no misorientation or low-angle grain boundaries, as determined by selective are diffraction and microstructural analysis via transmission electron microscopy. Similar results have been achieved for $Al_xGa_{1-x}N$ without the use of an AlN buffer layer. The stacking fault density was also very low. The dislocation density of the $Al_xGa_{1-x}N$ films at the SiC interface appeared similar to GaN films deposited on high temperature (HT) buffer layers[8,9]. The dislocation densities of the GaN and $Al_xGa_{1-x}N$ films decreased rapidly as a function of thickness; only threading dislocations which result from misfit dislocations at the interface persisted through the film.

The surfaces of the GaN and $Al_xGa_{1-x}N$ films exhibited a slightly mottled appearance as a result of the step and terrace features on the growth surface of the 6H-SiC(0001) substrates. Random pinholes, caused by incomplete coalescence of the two dimensional islands which occurred as an intermediate growth stage between the initial nucleation and the final layer-by-layer growth stage representative of the majority of the film, were also observed. An increasing number of pinholes appeared on

the surface of $Al_xGa_{1-x}N$ compositions where $x > 0.5$. The pinhole density was decreased by increasing the growth temperature to enhanced surface mobility of the adatoms. The DCXRC measurements taken on GaN and $Al_xGa_{1-x}N$ films revealed the FWHM of the (0002) reflections to be as low as 58 and 186 arcsec, respectively.

The low-temperature (8K) PL spectra of the undoped GaN films revealed an intense near band-edge emission at 3.466 eV, which has been attributed to an exciton bound to a neutral donor[17,18]. The FWHM value of this peak was 4 meV. Also, a less intense peak was observed at higher energies (3.472 eV) which is attributed to free excitonic recombination. The low-temperature (4.2K) CL spectra of the undoped $Al_xGa_{1-x}N$ films for compositions in the range of $0.05 \leq x \leq 0.96$ revealed an intense near band-edge emission which has been attributed to an exciton bound to a neutral donor (I_2-line emission)[17,18]. Broadening of this emission is attributed to both exciton scattering in the alloys as well as small variations in alloy composition in the film. The lowest FWHM value observed in the $Al_xGa_{1-x}N$ alloys was 31 meV. Strong defect peaks, previously ascribed to donor-acceptor pair recombination[19], were observed at midgap energies. The broad peak centered at 545 nm (2.2 eV) for GaN, commonly associated[20] with deep-levels (DL) in the bandgap, was also observed; however, these emissions shifted sublinearly with changing composition. The nature of this behavior is under investigation.

The compositions of the $Al_xGa_{1-x}N$ films were determined using EDX, AES and RBS. Standards of AlN and GaN grown in the same reactor under similar conditions were used for the EDX and AES analyses. After carefully consideration of the errors (±2 at.%) involved with each technique, compositions were assigned to each film. The data from EDX and AES measurements showed excellent agreement. The RBS data did not agree as well with the other two techniques due to small compositional variations through the thickness of the film. Simulation of the composition determined by RBS was conducted only on the surface composition.

These compositions were compared with their respective CL emission peaks and bandgap as determined by SE. Using a parabolic model, the functional relationships between I_2-line emission energy of the CL and the Al mole fraction for $0 \leq x \leq 0.96$ is shown in **Figure 9** and expressed analytically as

$$E_{I2}(x) = 3.47 + 0.64x + 1.78x^2 \qquad (1)$$

Clearly, this shows a negative deviation from a linear fit. This is in general agreement with earlier research over a smaller range of x by other investigators[16,17].

D. Selective Growth and Lateral Growth

The prismatic morphology of the GaN and $Al_{0.2}Ga_{0.8}N$ stripes deposited within the various window widths of the SiO_2 masks was observed using scanning electron microscopy. Micrographs of these results are

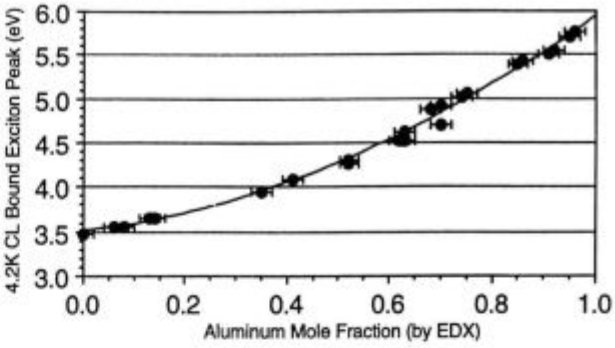

Figure 9: Low-temperature (4.2K) CL emissions of $Al_xGa_{1-x}N$ films as a function of aluminum mole fraction

Slika 9: Nizko temperaturni (4.2K) CL emisije $Al_xGa_{1-x}N$ filmov v odvisnosti od molarnega deleža AlN

shown in **Figure 10**. Both materials exhibited $(1\bar{1}00)$ side facets and ridge lines (i.e., no truncation) when deposited on the 3 µm-wide SiO_2 windows. Truncated prismatic growth with (0001) top facets and $(1\bar{1}01)$ side facets was observed on stripe patterns with widths ≥ 5 µm. Polycrystalline islands of $Al_XGa_{1-X}N$ nucleated on the SiO_2 mask because of the chemical interaction between Al and SiO_2 [20]. There was no significant difference in the final growth morphologies between the GaN and the $Al_{0.2}Ga_{0.8}N$ patterns, except for a slight roughening of the $(1\bar{1}01)$ facets of the latter. This roughening is believed due to the changes in the gas flow dynamics caused by the formation of the polycrystalline islands. No excessive growth was observed along the top edges of the truncated stripes, as shown in **Figure 11**; the (0001) top facets were very smooth and flat regardless of the width of these stripes. This suggests that the low growth pressure reduced the lateral vapor phase diffusion of the reactive species over the mask to the window region relative to that observed in related research conducted at one atmosphere[21]. The large ratio (=0.5) of the window-to-mask area may have also contributed to the perfection of the stripes, since lower values of this ratio were observed[22] to induce marked growth and rounding of the top edges at one atmosphere in GaAs, reportedly as a result of increased lateral vapor diffusion.

An increase in the flow rate of TEG resulted in a decrease in the area of the (0001) top facets and the development of $(1\bar{1}01)$ side facets. This behavior supports the model[23] that the resulting morphology of the selectively grown GaN depends on the balance between the incoming vapor flux on the (0001) top facets and the rate of diffusion on the (0001) surface to the $(1\bar{1}01)$ side facets. Increased exposure of the former to the TEG via an increase in the flow rate causes the growth rate of these facets to become faster than the latter.

The optimum conditions for the selective growth of the GaN pyramids on the circular patterns were based on the selective growth conditions on the stripe patterns. Each pyramid contained six $(1\bar{1}01)$ side facets. The growth rate of these pyramids was strongly dependent

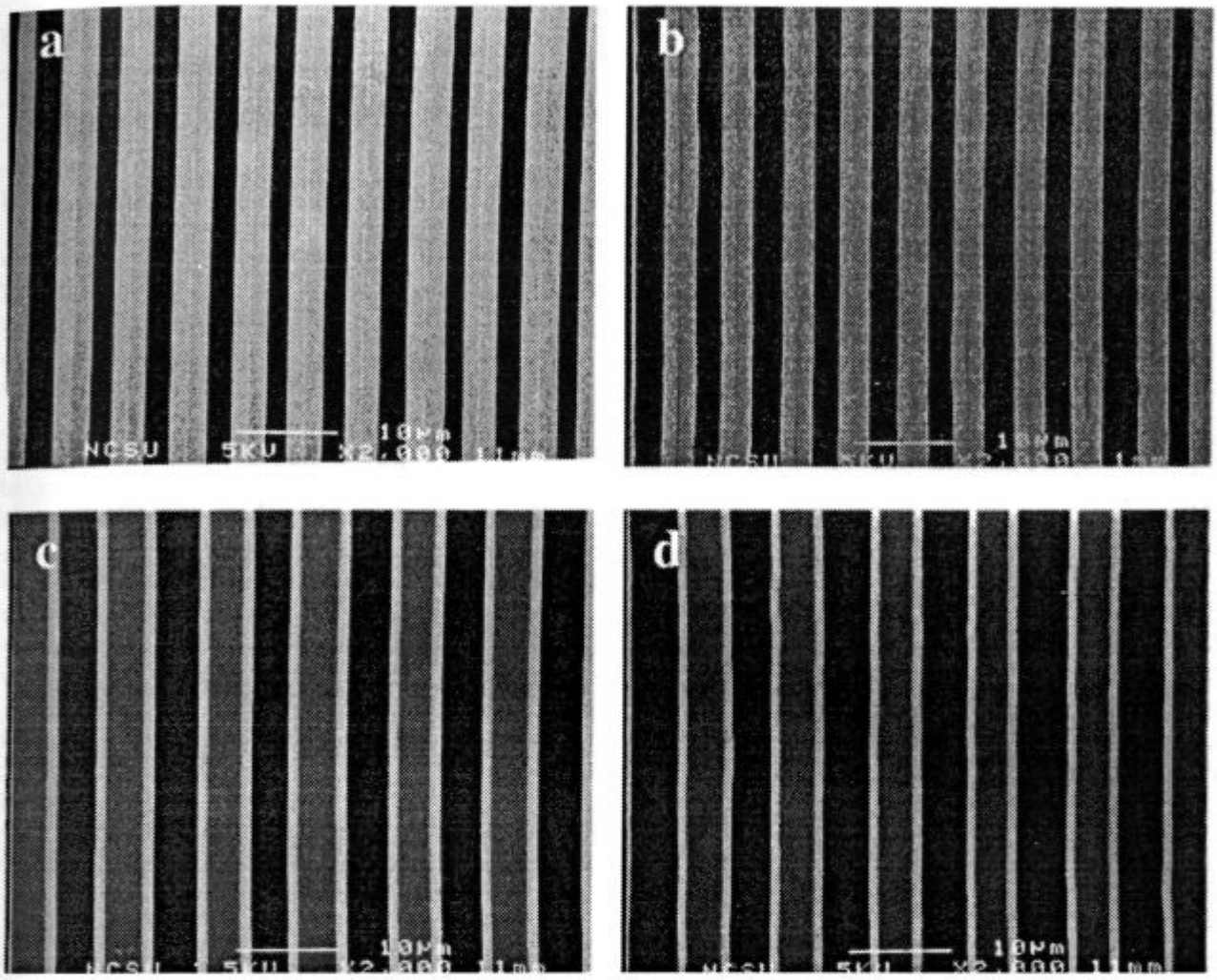

Figure 10: Secondary electron microscopy micrographs of GaN(left) and $Al_{0.2}Ga_{0.8}N$(right) stripes selectively grown at 1050°C and having initial SiO_2 widths of (a and b) 3 µm and (c and d) 5 µm

Slika 10: SEM posnetki GaN (levo) in $Al_{0.2}Ga_{0.8}N$ (desno) trakov selektivno zrastli pri 1050°C z začetno širino SiO_2 (a in b) 3 µm in (c in d) 5 µm

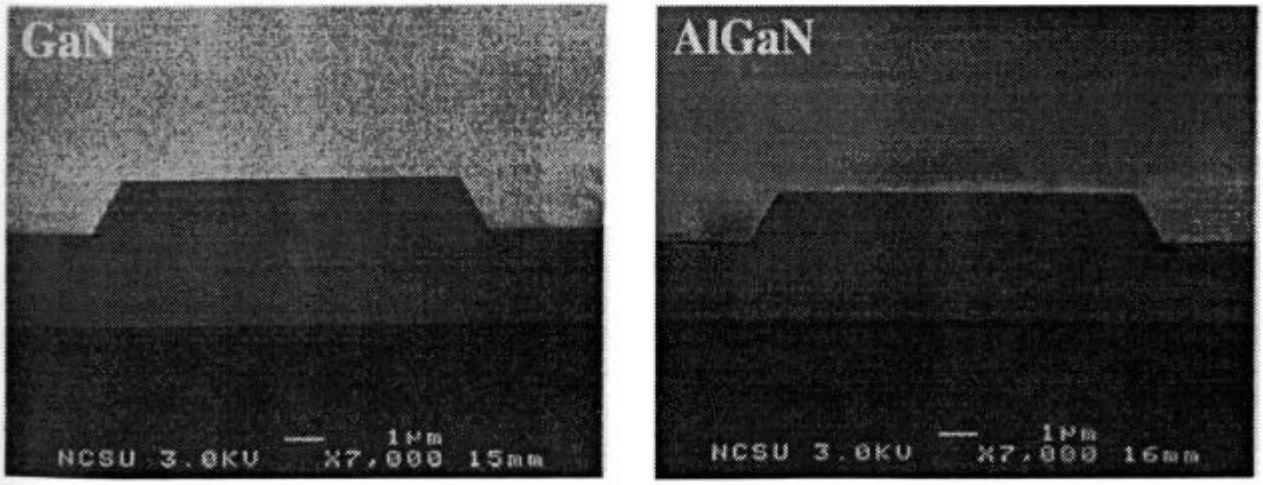

Figure 11: Secondary electron microscopy micrographs of 10 µm wide GaN and $Al_{0.2}Ga_{0.8}N$ stripes selectively grown at 1050°C with 10 µm wide SiO_2 windows

Slika 11: SEM posnetki 10 µm širokih GaN in $Al_{0.2}Ga_{0.8}N$ lamel selektivno zraščeni pri 1050°C z 10 µm širokimi SiO_2 okni

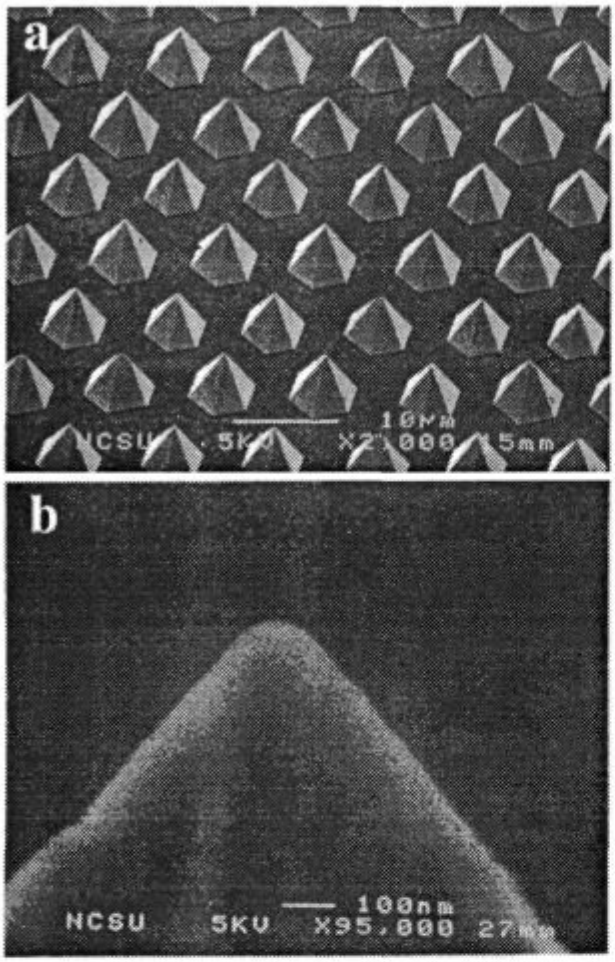

Figure 12: (a) SEM micrograph of a Si-doped GaN hexagonal pyramid array grown at 1000°C. (b) High magnification SEM image of the apex of a hexagonal pyramid having a tip radius of 100 nm
Slika 12: SEM posnetek heksagonalne združbe piramid GaN dopiranega s Si zrastlih pri 1000°C. (b) SEM posnetek vrha heksagonalne piramide z radijem konice 100 nm

upon the ratio of the window-to-mask area in the patterned region as well as the selective growth conditions. The average diagonal width of the pyramids was 7.7 μm using a ratio of 0.1. However, increasing the ratio to 0.23 resulted in an average diagonal width of 5.7 μm for the same growth conditions. These results indicate that the lateral diffusion of the reactive species from the mask to the window area is also an important factor for the successful fabrication of the GaN pyramids. As shown in **Figure 12(a)**, the growth of an uniform array of Si-doped GaN pyramids in a 0.5x0.5 mm^2 area was achieved. The high magnification SEM image shown in **Figure 12(b)** reveals that the tip radius of the pyramids was less than 100 nm.

The field emission current from the Si-doped GaN pyramid arrays was measured as a function of the anode voltage. The I-V curve in **Figure 13** shows a turn-on voltage of ≈680V for a current of 10.8 nA at a distance of 27 μm between the pyramid array and the anode. This turn-on voltage corresponds to a turn-on field of 25 V/μm. Using the same system, a polycrystalline p-type diamond film (p = 2.5E17cm^{-3}) grown on Si(100) exhibited a turn-on field intensity of 27 V/μm. The Fowler-Nordheim (F-N) plot obtained from the I-V data was linear and, therefore, indicates that the emission occurred via electron tunneling through the GaN.

The morphologies of the GaN layers selectively grown on the stripe openings were a strong function of the growth temperature, the flow rates of TEG and the stripe orientation. Continuous 2 μm thick GaN layers were obtained using 3 μm wide stripe openings spaced 7 μm apart and oriented along <1$\bar{1}$00> **(Figure 14 (a))**. The growth parameters were 1100°C and a TEG flow rate of 26 mmol/min. Plan view SEM of the coalesced GaN layer revealed a microscopically flat and pit-free surface, as shown in **Figure 14 (b)**. Atomic force microscopy showed the surfaces of the laterally grown GaN layers to possess a terrace structure having an average step height of 0.32 nm. The average RMS roughness values of the regrown and overgrown layers were 0.23 nm and 0.29 nm, respectively.

The cross-sectional TEM micrograph presented in **Figure 15** shows a typical laterally overgrown GaN. Threading dislocations, originating from the GaN/AlN buffer layer interface, propagate to the top surface of the regrown GaN layer within the window regions of the mask. The dislocation density within these regions, calculated from plan view TEM micrographs is approximately 10^9 cm^{-2}. By contrast, there were no observable threading dislocations in the overgrown layer. Additional microstructural studies of the areas of lateral growth obtained using various growth conditions have shown that the overgrown GaN layers contain only a few dislocations.

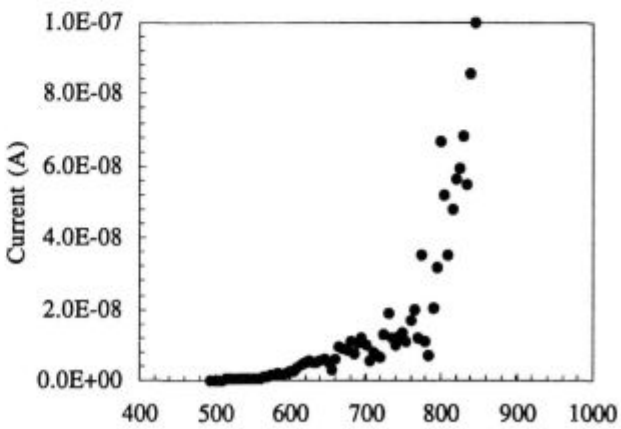

Figure 13: Emission current and anode voltage characteristics of Si-doped GaN hexagonal pyramid array shown in **Figure 12**
Slika 13: Karakteristike emisijskega toka in anodne napetosti heksagonalnih piramid s Si dopiranega GaN s **slike 12**

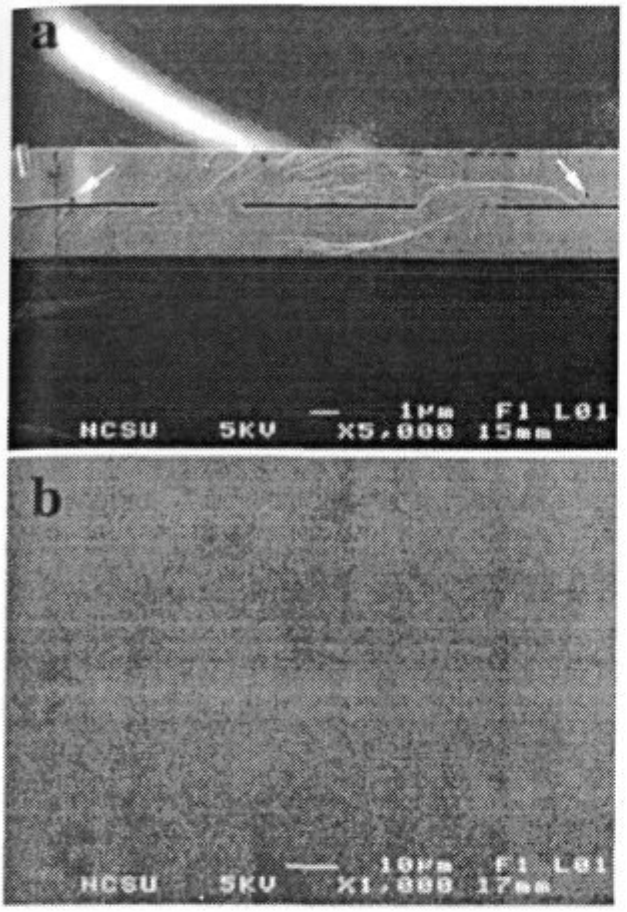

Figure 14: (a) Cross-section and (b) surface SEM micrographs of coalesced GaN layers grown on 3 μm wide and 7 μm spaced stripe openings, respectively, oriented along <1$\bar{1}$00>
Slika 14: Posnetki (a) prereza in (b) površina kolesciranih slojev GaN, ki so zrastli na 3 μm širokih 7 μm med seboj oddaljenih lamelnih odprtinah orientiranih vzdolž <1$\bar{1}$00>

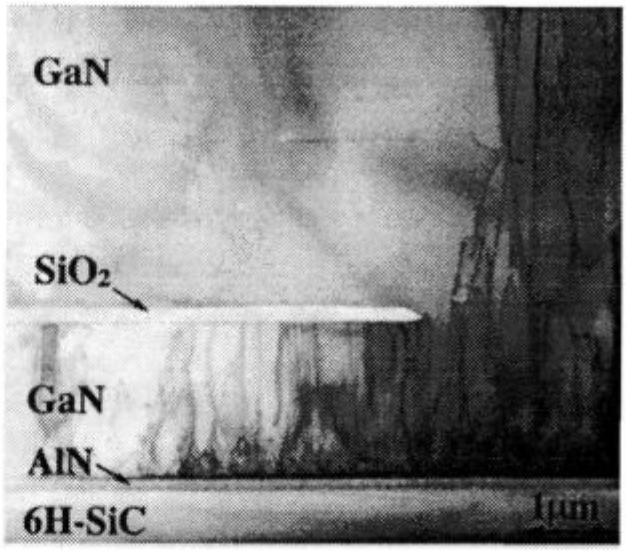

Figure 15: Cross-section TEM micrograph of a section of a laterally overgrown GaN layer on an SiO_2 mask region
Slika 15: TEM posnetek prereza lateralno zrastlega GaN sloja na področju SiO_2 maske

4 CONCLUSIONS

Growth of bulk, wurtistic GaN crystals to 3 mm length was achieved at a substrate temperature and pressure of 1100°C and 760 Torr, respectively, via sublimation of GaN pellets produced by uniaxial cold pressing of GaN powder. The concentrations of H, C and Si were ≤ 10^{16} atoms/cm^3 and the concentration of O was ≈ $3x10^{18}$ atoms/cm^3. Strong, sharp near band edge (bound exciton) emission was observed in the PL spectra of these crystals. No yellow emission was observed. An optical absorption edge of ≈ 370 nm and 75% transmission was determined. The Raman spectrum showed narrow and well positioned peaks.

Seeded bulk growth of single crystalline AlN (001) platelets was achieved on 6H-SiC (0001) substrates in the temperature range of 1950-2250°C at 500 torr of N_2. Color variations were observed above 2150°C and linked to the incorporation of Si and C from the substrate and the growth crucible. The results of TEM and XRD analyses revealed low densities of line and planar defects and the absence of residual stress in the grown crystals. No misoriented grains or twinned regions were observed. Very smooth surfaces (RMS≈6 Å) were observed via AFM.

Monocrystalline GaN and $Al_xGa_{1-x}N$(0001) ($0.05 \leq x \leq 0.96$) thin films, void of oriented domain structures and associated low-angle grain boundaries, were obtained via MOVPE on α(6H)-SiC(0001) wafers. A 1000Å high temperature (HT) AlN buffer layer was employed for the GaN deposition while $Al_xGa_{1-x}N$ was deposited directly on 6H-SiC. Double-crystal XRC measurements showed FWHM values as low as 58 and 186 arc sec for the GaN(0002) and $Al_xGa_{1-x}N$(0002) reflections. Photoluminescence spectra of GaN showed bound and free excitonic recombination. Spectra obtained via CL of $Al_xGa_{1-x}N$ showed strong near band-edge emissions with FWHM values as low as 31 meV.

The selective growth of GaN and $Al_{0.2}Ga_{0.8}N$ has been achieved on striped and circular patterned GaN/AlN/6H-SiC(0001) multilayer substrates. Prismatic morphology with well-defined (1$\bar{1}$01) side facets was observed on 3 μm wide stripes for both materials. Truncated prismatic growth with smooth, flat (0001) top facets and (1$\bar{1}$01) side facets were obtained on stripe patterns with widths ≥ 5 μm. Uniform hexagonal pyramid arrays of Si-doped GaN were successfully grown on circular patterns having diameters of 5 μm. Field emission measurements of these arrays showed a turn-on field of 25 V/μm and an associated emission current of 10.8 nA at an anode-to-pyramid array distance of 27 μm. Lateral growth and coalescence over the SiO_2 masks have been achieved using stripes oriented along <1$\bar{1}$00>. A density of ≈10^9 cm^{-2} threading dislocations, originating from the

underlying GaN/AlN interface, were contained in the GaN grown in the window regions. The overgrowth regions contained a very low density of dislocations.

ACKNOWLEDGEMENTS

The authors express their appreciation to Cree Research, Inc. for the SiC wafers. This work was supported by the Office of Naval Research under research contracts N00014-96-1-0765 and N00014-92-J-1477. R. Davis was supported in part by the Kobe Steel, Ltd. Professorship.

5 REFERENCES

[1] M. T. Duffy, in *Heteroepitaxial Semiconductors for Electronic Devices*, G. W. Cullen and C. C. Wang, Eds., Spinger Verlag, Berlin 1978 pp. 150-181

[2] R. F. Davis, *Proc. IEEE 79* (1991) 702

[3] S. Strite and H. Morkoç, *J. Vac. Sci. Technol. B*, 10, (1992) 1237

[4] J. H. Edgar, *J. Mater. Res.*, 7 (1992) 235

[5] J. L. Shaw, H. F. Gray, K. L. Jensen and J. M. Jung, *J. Vac. Sci. & Technol.*, B14 (1996) 2072

[6] R. J. Nemanich, M. C. Benjamin, S. P. Bozeman, M. D. Bremser, S. W. King, B. L. Ward, R. F. Davis, B. Chen, Z. Zhang and J. Bernholc, *Proc. Mat. Res. Soc.*, 395 (1996), 777

[7] M. C. Benjamin, C. Wang, R. F. Davis and R. J. Nemanich: *Appl. Phys. Lett.*, 64 (1994) 3288

[8] T. W. Weeks, Jr., M. D. Bremser, K. S. Ailey, E. P. Carlson, W. G. Perry, R. F. Davis, *Appl. Phys. Lett.*, 67 (1995) 401

[9] T. W. Weeks, Jr., M. D. Bremser, K. S. Ailey, W. G. Perry, E. P. Carlson, E. L. Piner, N. A. El-Masry, R. F. Davis, *J. Mat. Res.*, 4 (1996) 1011

[10] C. M. Balkas and R. F. Davis, *J. Am. Ceram. Soc.*, 79 (1996) 2309

[11] Cree Research, Inc., 2810 Meridian Parkway, Suite 176, Durham, NC 27713

[12] O. H. Nam, M. D. Bremser, T. S. Zheleva and R. F. Davis, to be published in *Appl. Phys. Lett.*, 71 (1997), 2638

[13] S. Sakai, S. Kurai, T. Abe and Y. Naoi, *Jpn. J. Apl. Phys.*, 35 (1996) L77

[14] L. Bergman and R. J. Nemanich, *Annu. Rev. Mater. Sci.*, 26 (1996) 551

[15] J. F. Muth, Private communication, North Carolina State University (1997)

[16] T. W. Weeks, Jr., D. W. Kum, E. Carlson, W. G. Perry, K. S. Ailey and R. F. Davis, *Second International High Temperature Electronics Conference*, Charlotte, NC, June 5-10 (1994)

[17] M. R. H. Khan, Y. Koide, H. Itoh, N. Sawaki, I. Akasaki, *Solid State Commun.*, 60 (1986) 753

[18] B. V. Baranov, V. B Gutan, U. Zhumakulev, *Sov. Phys.-Semicond.*, 16 (1982) 819

[19] R. Dingle and M. Ilegems, *Solid State Commun.*, 9 (1971) 175

[20] W. Götz, N. M. Johnson, R. A. Street, H. Amano and I. Akasaki, *Appl. Phys. Lett.*, 66 (1995) 1340

[21] Y. Kato, S. Kitamura, K. Hiramatsu and N. Sawaki, *J. Cryst. Growth*, 144 (1994) 133

[22] K. Yamaguchi and K. Okamoto: *Jpn. J. Appl. Phys.*, 32 (1993) 1523

[23] S. Kitamura, K. Hiramatsu and N. Sawaki, *Jpn. J. Appl. Phys.*, 34 (1995) 1184